



Chen, Jun, Zhang, Honggang, Liu, Lixuan, Zhang, Jing, Cooper, Mick, Mortimer, Robert ORCID logoORCID: <https://orcid.org/0000-0003-1292-8861> and Pan, Gang (2021) Effects of elevated sulfate in eutrophic waters on the internal phosphate release under oxic conditions across the sediment-water interface. Science of the Total Environment, 790. p. 148010.

Downloaded from: <https://ray.yorks.ac.uk/id/eprint/5347/>

The version presented here may differ from the published version or version of record. If you intend to cite from the work you are advised to consult the publisher's version:  
<http://dx.doi.org/10.1016/j.scitotenv.2021.148010>

Research at York St John (RaY) is an institutional repository. It supports the principles of open access by making the research outputs of the University available in digital form. Copyright of the items stored in RaY reside with the authors and/or other copyright owners. Users may access full text items free of charge, and may download a copy for private study or non-commercial research. For further reuse terms, see licence terms governing individual outputs. [Institutional Repositories Policy Statement](#)

# RaY

Research at the University of York St John

For more information please contact RaY at  
[ray@yorks.ac.uk](mailto:ray@yorks.ac.uk)

1   **Effects of elevated sulfate in eutrophic waters on the internal**  
2   **phosphate release under oxic conditions across the sediment-water**  
3   **interface**

4       Jun Chen<sup>1, 2</sup>, Honggang Zhang<sup>1, 5</sup>, Lixuan Liu<sup>6</sup>, Jing Zhang<sup>1</sup>, Mick  
5       Cooper<sup>3, 4</sup>, Robert J. G. Mortimer<sup>7, 8</sup>, Gang Pan<sup>1, 3, 4, 8\*</sup>

6       <sup>1</sup>*Research Center for Eco-Environmental Sciences, Chinese Academy of Sciences, Beijing 100085, China*

7       <sup>2</sup>*University of Chinese Academy of Sciences, Beijing, 100049, China*

8       <sup>3</sup>*School of Animal, Rural and Environmental Sciences, Nottingham Trent University, Brackenhurst Campus, NG25*  
9       *0QF, UK*

10      <sup>4</sup>*Integrated Water-Energy-Food Facility (iWEF), Nottingham Trent University, Nottinghamshire NG25 0QF, UK*

11      <sup>5</sup>*Yangtze River Delta Branch, Research Center for Eco-Environmental Sciences, Chinese Academy of Sciences, Yiwu*  
12      *322000, China*

13      <sup>6</sup>*High-Tech Research Institute Beijing University of Chemical Technology Beijing, China*

14      <sup>7</sup>*York St John University, Lord Mayor's Walk, York YO31 7EX, UK*

15      <sup>8</sup> *Nanjing Xianglai Institute of Eco-environmental Science and Technology, Nanjing 210046, China*

16

17      \* *Corresponding authors: gang.pan@ntu.ac.uk (Gang Pan)*

## 18    **Abstract**

19        Eutrophication in freshwater environments may be enhanced by the elevation of  
20    sulfate in waters, through the release of internal phosphorus (P) from anoxic sediments.  
21    However, the influence of increasing but modest sulfate concentrations (less than 3,000  
22     $\mu\text{M}$ ) on P release under oxic conditions across the sediment-water interface (SWI) in  
23    **eutrophic freshwater** is poorly understood. In this study, the profiles of P, iron (Fe), ~~and~~  
24    sulfur (S) **and physicochemical parameters** were measured in a simulated lacustrine  
25    system with varying concentrations of sulfate (970-2,600  $\mu\text{M}$ ) **in overlying water**. The  
26    results indicated that elevated concentrations of sulfate increased the soluble reactive P  
27    in overlying waters under oxic conditions across the SWI. A 100  $\mu\text{M}$  increase of sulfate  
28    was found to induce a  $0.128 \text{ mgm}^{-2}\text{d}^{-1}$  increase of P flux from surface sediments into  
29    overlying waters under oxic conditions. Higher sulfate concentrations in the overlying  
30    waters increased the concentrations of labile S(-II) in the deep sediments, due to sulfate  
31    penetration and subsequent reduction to S(-II). We also found the fluxes of labile Fe  
32    and P from deep to surface sediment were both positive and greater than the  
33    corresponding fluxes from surface sediment to the overlying water, suggesting that  
34    reduction of P-bearing Fe(III)(oxyhydr)oxides in deep anoxic sediment acted as a major  
35    source of internal P release. In addition, the upward flux of Fe(II) was significantly  
36    lower under higher sulfate conditions, indicating that the Fe(II) flux could be **blocked**  
37    **mitigated** by formation of Fe(II) sulfides in the deep sediment. Under these conditions,  
38    less Fe(II) from deep sediments could be re-oxidized and combine with P in the surface,

oxic sediment, thereby reducing the retention capacity for P and leading to higher release of internal P to the water column.

**Key words:** Eutrophication, Internal P loading, Sulfate, Freshwater, DGT

## **1. Introduction**

Eutrophication and the consequent formation of harmful algal blooms (HABs) represents a global challenge and poses serious threats to ecosystem services and human health (Conley et al. 2009, Paerl et al. 2011, Smith 2003). Phosphorus (P) is regarded as one of the primary limiting factors for the control of eutrophication in freshwater (Carpenter 2008, Schindler et al. 2008). Measures aimed at reducing inputs of external phosphorus have resulted in large-scale declines of phosphorus concentrations in many water bodies around the world (Huser et al. 2018, Tong et al. 2017). However, lakes typically show a delayed recovery in response to decreasing external P loads (Coveney et al. 2005), due to release of internal P from sediments (Paytan et al. 2017). Thus, understanding the processes of P release from sediments is important for the successful management of eutrophic waters.

The process of internal P release is influenced by many factors, such as temperature, pH and redox conditions (Christophoridis and Fytianos 2006). Iron (Fe) is a redox-sensitive element and the biogeochemical cycling of Fe regulates the mobility of internal phosphorus (Mortimer 1942). Under anoxic conditions, the reductive dissolution of P-bearing Fe(III)(oxyhydr)oxides is recognized as a major mechanism for internal P release (Rydin 2000). However, comparison of 23 different aquatic

60 systems did not show a strong correlation between internal P release rate and the bottom  
61 water oxygen concentration (Caraco et al. 1989). In addition, the sulfate concentration  
62 of the water was regarded as an extremely important variable controlling sediment P  
63 release in multiple systems, and showed a strong correlation with P release rate under  
64 both oxic and anoxic conditions (Caraco et al. 1989). Thus, the amount of P released  
65 from the sediment depended on the availability of sulfate (Caraco et al. 1989).

66 It has been found that the sulfide produced during sulfate reduction promote P  
67 mobilization from marine sediment through its dual effect on the cycling of Fe  
68 (Lehtoranta et al. 2009, Roden and Edmonds 1997, Rozan et al. 2002). Firstly, sulfide  
69 is a powerful reductant for the reduction of solid Fe(III) minerals to dissolved Fe(II)  
70 ion with concurrent P release (Bostrom et al. 1988). Secondly, sulfide could displace P  
71 from solid-phase Fe(II)-P compounds and trap the dissolved Fe(II) ion to iron sulfide  
72 precipitation (Roden and Edmonds 1997), which significantly promotes P release and  
73 reduces P retention capacity (Lehtoranta et al. 2009). For freshwater lakes with low  
74 concentrations of sulfate, it is commonly accepted that sulfate has slight effect on  
75 internal P release and Fe cycling (Caraco et al. 1989, Hansel et al. 2015). During recent  
76 decades, sulfate concentrations have increased in freshwater systems due to acid  
77 deposition and industrial wastewater inputs (Yu et al. 2013, Zak et al. 2006). For  
78 example, sulfate concentration in Lake Taihu has undergone a rapid increase ( $>12 \mu\text{M}$   
79  $\text{L}^{-1}\text{y}^{-1}$ ) over the past 60 years and now attains concentrations close to  $1,000 \mu\text{M}$  (Yu et  
80 al. 2013). Caraco et al. (1989) proposed that freshwater systems with intermediate

sulfate concentration (~100-300  $\mu$ M sulfate) tended to have high P release rates under anoxic condition. Some researchers showed that increasing sulfate levels could significantly promote the internal P release in freshwater lakes under anoxic conditions (Chen et al. 2016a, Roden and Edmonds 1997, Zhao et al. 2019). So far, anoxic conditions in the bottom water could be considered as an essential prerequisite for sulfate-stimulated release of P from sediments in freshwater systems.

Under natural conditions, oxygen distribution across the sediment-water interface (SWI) in shallow freshwater lakes, like Lake Taihu in China, is heavily influenced by hydrodynamic disturbance, accelerating the oxygen diffusion rate from the atmosphere to the water column (Chatelain and Guizien 2010). Thus, anoxia in bottom waters is hardly persistent during most seasons, except in the summer months. In the oxygenated water column and oxic surface sediments, Fe(II) may be rapidly converted to Fe(III)(oxyhydr)oxides, which provide fresh adsorption sites on which to retain available P (Mortimer 1942). Although oxic conditions across the SWI may increase the P adsorption capacity in surface sediment, P release is still observed in some oxic bottom waters (Gächter and Müller 2003, Kraal et al. 2013). These observations suggest that other mechanisms may also affect internal P release. For example, P can be released by dissolution of vivianite by interaction with hydrogen sulfide in deep sediments where oxygen cannot diffuse (Gächter and Müller 2003). Thus, higher concentrations of hydrogen sulfide in deep sediments may influence P release from surface sediments under oxic SWI conditions. Hansel et al. (2015) found that even when the sulfate

concentration was as low as 200  $\mu\text{M}$ , sulfate reduction was still a dominate force for the reduction of Fe(III) oxide. Increasing concentration of the sulfate in freshwater lakes has the potential to promote the mobilization of P through its effect on the cycling of iron under oxic condition across the SWI. However, to date no quantitative analysis has been undertaken on the contribution of elevated sulfate in shallow freshwaters to internal P release under oxic SWI conditions. Work to date has only been undertaken on sulfate rich waters such as a lowland river (2,600-7,800  $\mu\text{M}$  sulfate) polluted by mining activities and an estuary (28,000  $\mu\text{M}$  sulfate) (Kraal et al. 2013, Zak et al. 2006), neither of which has wide applicability for freshwater systems. In addition, a comprehensive evaluation of the impact of sulfate on the dynamic cycling of S-Fe-P, and their interactions, is crucial to the understanding of how eutrophication conditions change with oxic-anoxic variations.

In this study, an incubation experiment was conducted in a continuous dynamic shallow water simulation system under three sulfate levels. Diffusive gradients in thin films (DGT) and microelectrode techniques were employed to collect the vertical dynamic features of labile of P, Fe, S, as well as the related environmental factors at a fine scale. Based on the DGT profiles, the apparent fluxes of labile P and Fe from both surface sediment to water, and from deep sediment to surface sediment, were calculated. The objective of the study was to explore the effects of elevated sulfate inputs to the water column under oxic SWI conditions on internal P release.

## 2. Materials and methods

### 2.1. Sample Collection

The sampling sites were in Meiliang Bay (120°9 E, 31°31 N), the northern part of Lake Taihu. Lake Taihu is the third largest freshwater lake in China and is experiencing eutrophication and algal blooms. Sulfate concentrations here have undergone a rapid increase over the past 60 years and now attain about 1,000  $\mu\text{M}$  (Yu et al. 2013). Sediments and lake water were collected from Lake Taihu using an Ekman grab sampler and Plexiglas hydrophore, respectively. The collected samples were transported to the laboratory immediately and stored at 4 °C for less than 24 h before pre-treatment.

### 2.2. Preparation of sediment-water columns

Sediments were sieved through a 0.5 mm pore-size mesh to remove occasional macrofauna and large particles, and then completely homogenized to eliminate the horizontal heterogeneity of the natural sediment (Ding et al. 2015, Zilius et al. 2016). The pre-treated sediments and overlying water (filtered with 0.45  $\mu\text{m}$  filters) were used to fill perspex cylinders (8.4 cm in diameter and 50 cm in height) and 48 cylinders were produced in this study. Each cylinder contained 20 cm of sediment and 25 cm of overlying water. This sediment pretreatment method has been used extensively in other incubation experiments focused on exchange across the SWI (Chen et al. 2016b, Sun et al. 2017, Wang et al. 2017).

### 2.3. Microcosm set-up

Water flow over sediment has a significant influence on oxygen consumption



(Higashino 2011) and water-sediment interaction (Qin et al. 2007), which play key roles in Fe-S-P cycling. Taking this into consideration, we designed a dynamic microcosm system. The microcosm system consisted of six units, each including a water reservoir tank (12.3 cm in diameter and 20 cm in height) and six perspex cylinders (Figure.S1a and b). All of the cylinders were sealed with rubber plugs and silicone sealant. A micro pump and an aeration unit were installed in each reservoir tank (Figure.S1c). Water from each of the reservoir tanks was separately pumped into the inlet of the first cylinder of each unit, at 5 cm above the surface of sediment, and flowed out through the outlet of the cylinder, into the inlet of the next cylinder in the unit. All six cylinders in one unit were connected in series via their inlets and outlets, to simulate the regular water movement in shallow lakes and uniform initial conditions among cylinders. The water in the final cylinder of a unit flowed into the reservoir tank of the next unit. Water in each reservoir tank was initially sparged with N<sub>2</sub> at a flow rate of 0.4 L min<sup>-1</sup> for 24 h to remove oxygen from each unit and then air was pumped into each tank for 5 min h<sup>-1</sup> to maintain the oxic environment across the SWI. The pre-incubation period lasted for 2 weeks.

At the end of pre-incubation, the concentrations of dissolved oxygen (DO), redox potential (Eh), DGT-labile P and Fe, and the soluble reactive P (SRP) in water-sediment profiles were measured from three randomly selected cylinders (Figure.S2). The profiles exhibited very consistent distributions for all the parameters, suggesting that the sediment was homogeneous in chemical distribution across different cylinders prior

to the main experiments.

#### *2.4. Incubation Experiment*

After pretreatment, the water in each of the final cylinders in a unit was directed back to that unit's own reservoir tank, and the entire microcosm was separated into eight independent units (Figure.S1b). We choose six units (36 cylinders) at random on which to perform the experiment.  $\text{Na}_2\text{SO}_{4(\text{S})}$  was subsequently dissolved in the corresponding reservoir tank to obtain the desired concentration values as follows: no addition (Control; group C), 1,770  $\mu\text{M}$  (low sulfate; group B), and 2,600  $\mu\text{M}$  (high sulfate; group A). Control group (970  $\mu\text{M}$ ) represented the background concentration of sulfate found in the water column of Lake Taihu. According the work of Caraco et al. (1989), the background concentration of sulfate ( $\sim 1000 \mu\text{M}$ ) in Lake Taihu is higher than the typical freshwater type ( $\sim 10\text{-}300 \mu\text{M}$ ). However, it is still much less sulfate rich than the sites (a lowland river (2,600-7,800  $\mu\text{M}$  sulfate) polluted by mining activities and an estuary (28,000  $\mu\text{M}$  sulfate)) studied previously (Kraal et al. 2013, Zak et al. 2006). As no mandatory standards of sulfate are declared for surface waters worldwide, we chose the quality standard of sulfate in drinking water (2,600  $\mu\text{M}$ ) in China (GB3838-2002, China) for the high sulfate group (group A), which was very close to lower limiting values of salt waters ( $\sim 3,000\text{-}30,000 \mu\text{M}$ ). The set value in group B was a median value between those for groups A and C. All three units were incubated at room temperature ( $20 \pm 2^\circ\text{C}$ ) for 45 days in the dark. Sampling was performed on the 10th, 20th, 30th, 32nd, 37th and 45th day after the onset of incubation.

## 2.5. Analyses of samples

On the planned sampling day, two columns for each treatment (treated as duplicates) were randomly selected for sediment and water sampling. The distribution of DO and Eh in water-sediment profiles were measured using needle-type microelectrodes (OX-100 and RD-100; Unisense, Denmark) and the overlying water was then collected. Subsequently, ZrO-Chelex and AgI DGT (Easysensor Ltd., China) probes bound back to back were inserted into the sediments (Han et al. 2015). 24 hours later, these DGT probes were retrieved from sediments for processing.

After that, the sediment samples were transferred to a glove box containing a dry nitrogen atmosphere and sliced at a vertical resolution of 1cm to a depth of 10cm. An aliquot of each sliced sediment sample was transferred to a 50 ml plastic centrifuge tube which was then capped, removed from the glove box and centrifuged at 2500 g for 30 min. After centrifugation, tubes were returned to the glove box to sample the pore water. The supernatant water in each centrifuge tube was dispensed via a 10 ml plastic syringe, fitted with a 0.45 $\mu$ m pore-size cellulose nitrate membrane filter, collected in a 5 ml plastic centrifuge tube, and finally stored at -20 °C. (Modified from Jilbert et al. (2011)).

The deployed ZrO-Chelex DGT was analyzed following the procedure detailed in Xu et al. (2013). The ZrO-Chelex gel was sliced at a resolution of 2 mm. Each sliced gel was sequentially eluted using HNO<sub>3</sub> and NaOH and the labile P and Fe in the eluates were determined using a microplate spectrophotometer (Multiskan FC; Thermo Scientific, Waltham, USA). The concentrations of labile S contained in the binding layer of the AgI DGT were determined by computer imaging densitometry (CID). The

image of the AgI gel was scanned using a flat-bed scanner (Canon 5600F, Canon Inc., Japan) at a resolution of 600 dpi (0.0423 mm×0.0423 mm) and then converted to grayscale intensities with Image J (Version 1.48, NIH, USA) (Ding et al. 2012). The concentrations of the labile P, Fe and S measured by the DGT were calculated by methods listed in the Supporting Information.

The concentration of SRP in the water was determined using the molybdenum blue method (Murphy and Riley 1962). The concentration of sulfate in water was measured using a turbid metric method (Tabatabai 1974).

## 2.6. Data processing

~~To reflect the diffusion direction of Fe and P across the sediment-water interface and oxic-anoxic interface.~~ To assess the effect of elevated sulfate in overlying water on internal P release under oxic condition across the SWI, the apparent fluxes at two depths were calculated in this study. Oxygen penetration depths in the sediment were measured as being less than 1cm (Fig.2.b). Therefore, this depth (-1 cm) was used to divide sediment profiles into surface oxic sediment and deeper anoxic sediment.

The ~~net~~-apparent fluxes of P and Fe at a specific depth were calculated from the DGT-labile P and labile Fe profiles using the following procedure:

(i)  $C = f(x)$ : get the regression equation between the measured concentrations (C) of P or Fe(II) and the corresponding depth (x).

So, the concentration gradients at the depth of i:  $\left. \frac{\partial C}{\partial x} \right|_{x=i} = f'(i)$  and the mean

concentration gradients from depth of m to depth of n:  $\left. \frac{\partial C}{\partial x} \right|_{mn} = \frac{\sum_{i=m}^n f'(i)}{m-n}$ . Based on the

depth-distributions of DGT-labile P and Fe, the concentration gradients were assessed

separately at the depths from 0 to 1 cm (overlying water), 0 to -1 cm (surface oxic sediment), -1 to -10 cm (deep anoxic sediment)

(ii) Taking the main mechanisms that could influence the internal P release into consideration, the ~~net~~ apparent fluxes of P or Fe(II) at the SWI were calculated as the sum of fluxes from surface sediment to the SWI, and from bottom water to the SWI using equation (1) (Ding et al. 2015, Gao et al. 2016).

$$F_0 = F_s + F_w = (-\phi D_s \frac{\partial c_s}{\partial x_s}) + (-D_w \frac{\partial c_w}{\partial x_w}) \quad (1)$$

Where  $F_0$  is the apparent flux ( $\text{mg m}^{-2}\text{d}^{-1}$ ) at the SWI.  $F_s$  and  $F_w$  represent the labile P or Fe fluxes from surface sediment to the SWI, and from bottom water to the SWI, respectively.  $\frac{\partial c_s}{\partial x_s}$  and  $\frac{\partial c_w}{\partial x_w}$  are the concentration gradients in surface sediment and

overlying water, respectively.  $\phi$  is the porosity in sediment.  $D_w$  is the diffusion coefficient in water ( $\text{cm}^2 \text{s}^{-1}$ ) calibrated by the actual temperature (Li and Gregory 1974).

The diffusion coefficient in sediment ( $D_s$ ) ( $\text{cm}^2 \text{s}^{-1}$ ) were calculated from the diffusion coefficient in water ( $D_w$ ) and porosity ( $\phi$ ) in sediment (Ullman and Aller 1982).  ~~$D_s$  is~~

~~the bulk sedimentary diffusion coefficient ( $\text{cm}^2 \text{s}^{-1}$ ) (Ullman and Aller 1982).  $D_w$  is the bulk sedimentary diffusion coefficient in water, and the porosity is  $\phi$  (Han et al. 2015,~~

~~Li and Gregory 1974) ;  $\frac{\partial c_s}{\partial x_s}$  and  $\frac{\partial c_w}{\partial x_w}$  are the concentration gradients in surface~~

~~sediment and overlying water, respectively.~~

(iii) Similarly, the ~~net~~ apparent fluxes of P or Fe(II) at 1 cm below the SWI (-1 cm) were calculated using equation (2)

$$F_1 = F_{s1} + F_{s2} = (-\phi D_{s1} \frac{\partial c_{s1}}{\partial x_{s1}}) + (-\phi_2 D_{s2} \frac{\partial c_{s2}}{\partial x_{s2}}) \quad (2)$$

Where  ~~$F_1$  is the apparent flux at 1 cm below the SWI (-1 cm).~~  $F_{s1}$  and  $F_{s2}$  represent the labile P or Fe fluxes from surface sediment to -1 cm, and from deep sediment to -1

cm, respectively.  $F_1$  is the and apparent flux at 1 cm below the SWI (-1 cm), which is the sum of  $F_{s1}$  and  $F_{s2}$ .  $D_{s1}$ ,  $\varphi_1$ ,  $\frac{\partial c_{s1}}{\partial x_{s1}}$ ,  $D_{s2}$ ,  $\varphi_2$ , and  $\frac{\partial c_{s2}}{\partial x_{s2}}$  were the mean values of sedimentary diffusion coefficients, porosity, and concentration gradient in surface sediment or deep sediment, respectively.

To comprehensively and quantitatively assess the concentration effect of sulfate on the internal P release in natural eutrophic waters (for instance, Lake Taihu in China), four linear regression equations were established, based on the functional relationships between the apparent fluxes ( $F_1$ ,  $F_0$  of labile Fe and P) and the concentrations of sulfate in overlying water. In addition, we extended the applied scope of the regression equations to predict the change of apparent fluxes of labile Fe and P over a wider concentration range of sulfate in freshwater systems. Here, four critical values for sulfate were determined by equations according to the following two scenarios:

Scenario 1: When the apparent diffusive flux of labile P or labile Fe across the SWI was zero ( $F_0=0$ )

Scenario 2: When the apparent diffusive fluxes of labile P or labile Fe were equal at the SWI and at 1 cm below the SWI ( $F_{10}=F_1-F_0$ ).

Based on the four critical values of sulfate derived here, we selected two of the critical values, which did not belong to the concentration range ( $\sim 3,000$ - $30,000 \mu\text{M}$ ) of salt waters (Caraco et al. 1989) and divided the concentration range ( $0$ - $3,000 \mu\text{M}$ ) into different parts.

All of the statistical analyses were performed using SPSS software (V25.0; SPSS, USA). The differences of DO, Eh, SRP in overlying water and oxygen penetration depth (OPD) in sediment between different treatments were determined by pairwise

comparisons using one-way analysis of variance (ANOVA) and the Duncans multiple range test were used to perform means comparison. Besides, the differences of labile S, labile Fe and labile P between different sampling times were also assessed. The differences between the mean values at significance probability ( $p$ )<0.05 were considered statistically significant. ~~One-way analysis of variance (ANOVA) was employed to detect differences of DO, Eh, SRP in overlying water and oxygen penetration depth (OPD) in sediment between different treatments. The difference of labile S, labile Fe and labile P between different sampling times were also assessed by ANOVA. A  $P$ <0.05 was considered significant.~~ The functional relationships between sulfate concentration in the overlying water and fluxes of labile Fe and P were established using linear fitting.

### 3. Results

#### 3.1. Vertical distribution of DO and Eh in sediment-water interface

Sulfate addition induced an apparent change in the DO profiles, including DO level (Figure.1a.) and DO penetration depth (Figure.2a) in the surficial sediment. The highest DO concentrations in bottom water and at each depth along the vertical water-sediment profiles were always found in the group A. The sediment oxygen concentrations in the group B were also higher at depths of -0.05 to -0.7 cm than those in the Control (Figure.1a). Furthermore, higher sulfate concentrations led to a significant increase in the vertical oxygen penetration depth (OPD) in the order of group A>group B>Control (one-way ANOVA,  $p$ <0.05) (Figure.2b).

The redox potential (ORP) showed a similar trend to DO (Figure.1b, Figure.2c). Sulfate addition significantly increased the ORP values in bottom water and followed the order group A>group B>Control (one-way ANOVA,  $p<0.05$ ). From the SWI to the depth of -3 cm, the ORP values in the group A and group B units were significantly higher than those in the Control group (one-way ANOVA,  $p<0.05$ ).

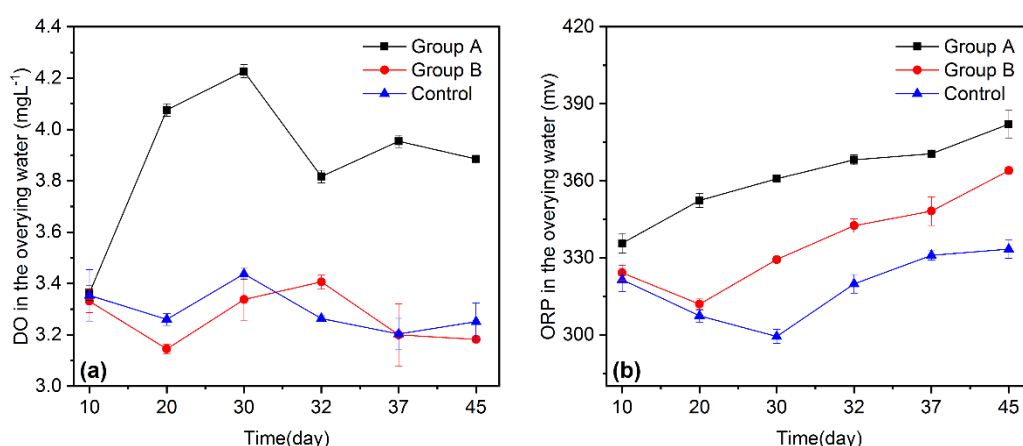


Figure 1. Variation of dissolved oxygen (DO) (a) and redox potential (ORP) (b) in bottom water from the three treatment groups during the 45-days incubation (data shown by mean  $\pm$  SD,  $n = 2$ ). Control: 970  $\mu\text{M}$ ; group B: low sulfate, 1,770  $\mu\text{M}$ ; group A: high sulfate, 2,600  $\mu\text{M}$ .

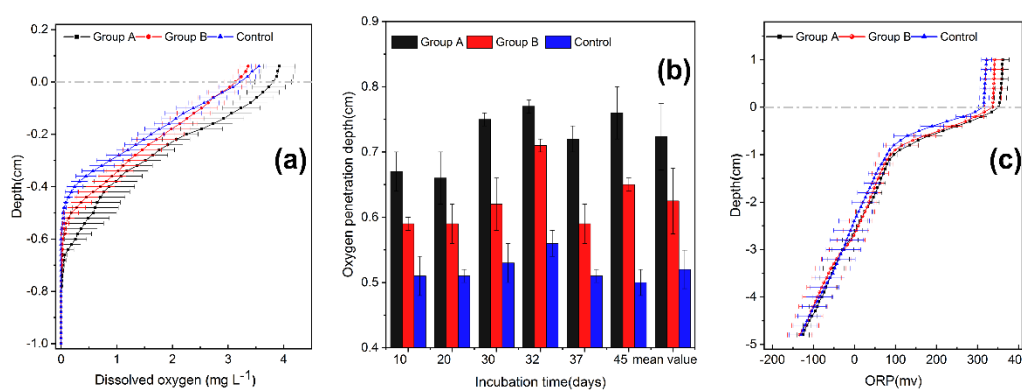


Figure 2. Dissolved oxygen profiles (DO) (a), oxygen penetration depth (OPD) (data shown by mean  $\pm$  SD,  $n = 2$ ) (b) and redox potential (ORP) profiles (c) from the three treatment groups (data of DO and OPD were shown by the mean values during the 45-days incubation period  $\pm$  SD,  $n=12$ ). The horizontal dashed line indicates the sediment-water interface (SWI). Control: 970  $\mu\text{M}$ ; group B: low sulfate, 1,770  $\mu\text{M}$ ; group A: high sulfate, 2,600  $\mu\text{M}$ .



### 3.2. Vertical distribution of sulfate and DGT-labile S in the sediment-water profiles

The concentrations of sulfate in overlying water were  $2,394 \pm 67$  in group A,  $1,658 \pm 33$  in group B, and  $911 \pm 55$   $\mu\text{M}$  in the Control (Figure. 3a). In all groups, the sulfate concentration in pore water decreased slightly with increase in sediment depth. In addition, the concentration of sulfate in pore water at each depth followed the order group A > group B > Control (Figure. 3a).

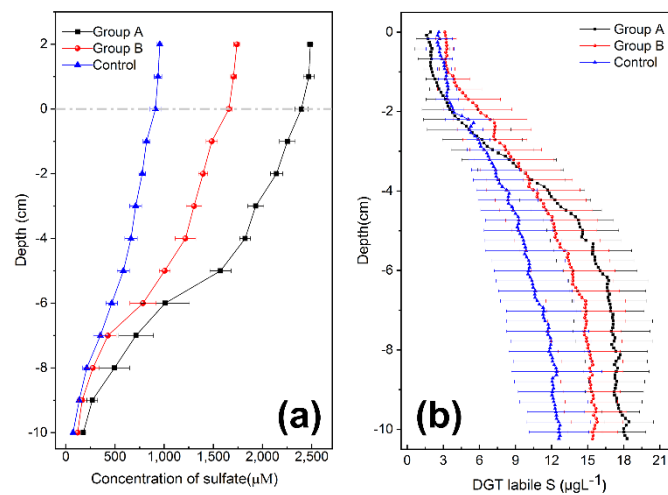


Figure 3. Changes in the concentration of sulfate with depth in the sediment-overlying water profiles (a) (data of sulfate was shown by the mean values of all sampling times during the 45-days incubation period  $\pm$  SD,  $n=12$ ), one-dimensional distributions of DGT-labile S in profiles as determined by AgI DGT (b) of different sulfate treatments (the data of labile S was shown by the mean values of all sampling times during the 45-days incubation period  $\pm$  SD,  $n=6$ ). The horizontal dashed line indicates SWI. Control:  $970$   $\mu\text{M}$ ; group B: low sulfate,  $1,770$   $\mu\text{M}$ ; group A: high sulfate,  $2,600$   $\mu\text{M}$ .

The labile S (Figure.3b) profiles exhibited a similar trend, increasing with depth in all three groups. Interestingly, lower concentrations of labile S in surface sediments were found in group A, except at day 20 (Figure.S4). The average concentrations of labile S within the depths from SWI to -3 cm in group A were lower than those in the

Control and group B (Figure.3b). However, that trend was reversed below -4 cm. The concentration of labile S in group A remained at a higher level in the deep sediment (below -3 to -4 cm) throughout the incubation period (Figure.S4). The average concentrations of labile S in group A from -4 to -10 cm were significantly higher than those in group B and the Control (one-way ANOVA,  $p<0.05$ ).

### 3.3. Vertical distribution of SRP in sediment-water profiles

Soluble reactive P (SRP) concentrations in the overlying water were significantly higher in the groups with the increasing sulfate concentration (one-way ANOVA,  $p<0.05$ ) and the average values followed the order: group A>group B>Control (Figure. 4 and Figure. S3). After the 30th day of incubation, the concentration of SRP in the pore water of sulfate addition groups (group A and B) was higher than the Control. On the 45th day of incubation, the average concentrations of SRP in pore water from SWI to -8 cm in group A and group B were 52.3% and 48.6% higher than the Control. However below -8 cm, no evident difference in concentrations of SRP was observed during 45-days incubation between the three groups (RSD=1.06 % in three groups).

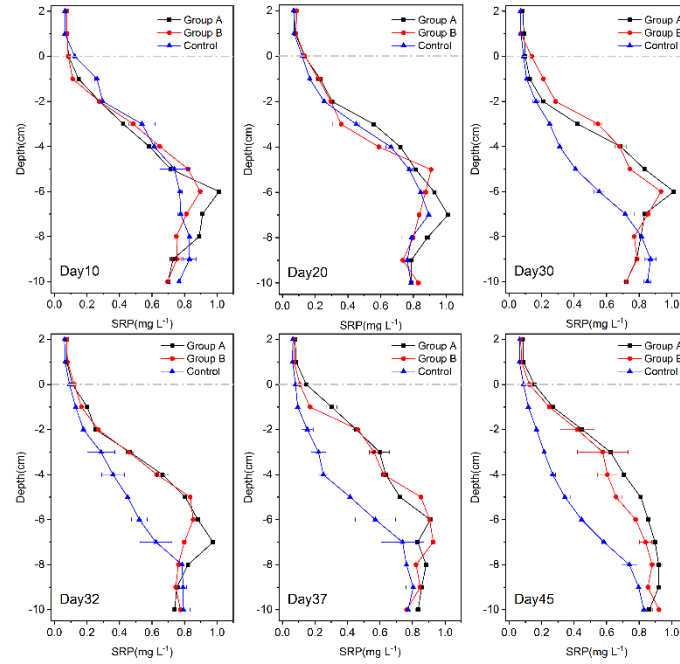


Figure 4. Changes of SRP (Soluble Reactive P) in the sediment-water profiles from the three treatment groups during the 45-days incubation period (data shown by mean  $\pm$  SD,  $n = 2$ ). The horizontal dashed line indicates the SWI. Control: 970  $\mu\text{M}$ ; group B: low sulfate, 1,770  $\mu\text{M}$ ; group A: high sulfate, 2,600  $\mu\text{M}$ .

### 3.4. Vertical distribution of DGT-labile Fe and P in sediment-water profile

The concentrations of labile Fe and P from the overlying water to the surface sediments (SWI to -1 cm) remained at relatively low values and increased until -10 cm sediment depth (Figure.5, Figure.S5 and Figure.S6). There was no significant difference for labile Fe and labile P between different sampling time (most of  $P > 0.05$ , the specific  $P$  values were listed in Table S2 and Table S3). Below -1 cm, the concentrations of labile Fe were varied from 0.24 to 2.71  $\text{mg L}^{-1}$  in group A, 0.13 to 2.82  $\text{mg L}^{-1}$  in group B and 0.10 to 3.21  $\text{mg L}^{-1}$  in the Control group, respectively. However, the concentrations of labile P were ranged between 0.01 to 0.33  $\text{mg L}^{-1}$  in group A, 0.03 to 0.30  $\text{mg L}^{-1}$  in group B and 0.01 to 0.28  $\text{mg L}^{-1}$  in the Control.

Statistically significant positive correlations between labile Fe and labile P in sediment were determined for each treatment ( $p < 0.001$ ) (Fig.S7).

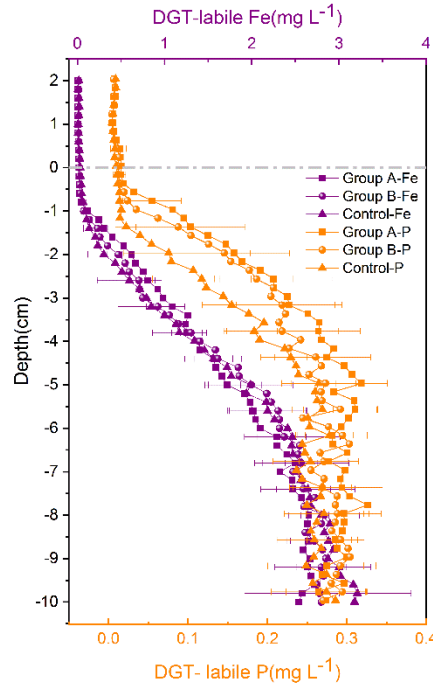


Figure 5. Effects of the sulfate addition on the one-dimensional vertical distribution of DGT-labile P and DGT-labile Fe in water-sediments profiles (data shown by the mean values of all sampling times during the 45-days incubation period  $\pm$  SD,  $n=6$ ). The horizontal dashed line indicates the sediment-water interface (SWI). Control: 970  $\mu\text{M}$ ; group B: low sulfate, 1,770  $\mu\text{M}$ ; group A: high sulfate, 2,600  $\mu\text{M}$ .

### 3.5. Apparent diffusive flux of $\text{PO}_4^{3-}$ and $\text{Fe(II)}$

The apparent diffusive fluxes of the target elements were calculated at SWI ( $F_0$ ) and 1 cm below the SWI ( $F_1$ ) based on Fick's first law (Figure. 6). The apparent fluxes of  $\text{PO}_4^{3-}$  and  $\text{Fe(II)}$  in the three groups across the SWI were all positive (effluxes) and ranged between 0.06 to 4.56  $\text{mgm}^{-2}\text{d}^{-1}$  and 1.41 to 5.32  $\text{mgm}^{-2}\text{d}^{-1}$ , respectively. The mean flux of  $\text{PO}_4^{3-}$  from the surface layer of sediment to water ( $F_0$ ) showed an increasing trend with the increase of sulfate in overlying water. The mean  $F_0$  of  $\text{PO}_4^{3-}$

374 in group A and group B were 5.5 and 1.9 times higher than that in the Control (0.40  
375  $\text{mgm}^{-2}\text{d}^{-1}$ ), respectively. The mean  $F_0$  of Fe(II) was lowest in group A (2.22  $\text{mgm}^{-2}\text{d}^{-1}$ )  
376 compared to that in group B (2.67  $\text{mgm}^{-2}\text{d}^{-1}$ ) and the Control (3.51  $\text{mgm}^{-2}\text{d}^{-1}$ ). The  
377 values of  $F_1$  in three groups were also positive and the fluxes of  $\text{PO}_4^{3-}$  and Fe(II) from  
378 deep sediment to surface sediment ranged between 0.88 to 4.00  $\text{mgm}^{-2}\text{d}^{-1}$  and 8.24 to  
379 30.53  $\text{mgm}^{-2}\text{d}^{-1}$ . Increasing sulfate in overlying water elevated the mean values of the  
380 flux of  $\text{PO}_4^{3-}$  from deep sediment to surface sediment ( $F_1$ ) with order of group A>group  
381 B>Control, whereas an opposite trend was observed for Fe(II).

382 The net flux ( $F_{10}$ ) of  $\text{PO}_4^{3-}$  and Fe(II) in the surface sediment was calculated by  
383 using the equation:  $F_{10}=F_1-F_0$ . The  $F_{10}$  of  $\text{PO}_4^{3-}$  and Fe(II) were all positive, except for  
384  $F_{10}$  of P in group A (highly variable, from 0.88 to -0.48  $\text{mgm}^{-2}\text{d}^{-1}$ ). The mean values of  
385  $F_{10}$  decreased with the increased sulfate in the overlying water. The retention  
386 efficiencies (defined by the quotient of  $F_1$  and  $F_{10}$ ) of P, diffused from deep to surface  
387 sediments in the Control group was about 70.1% and obviously higher than those in the  
388 group A and group B groups (3.6% and 22.1%, respectively). The retention efficiencies  
389 of Fe(II) were 78.5%, 80.4% and 80.8% in group A, group B and C, respectively.

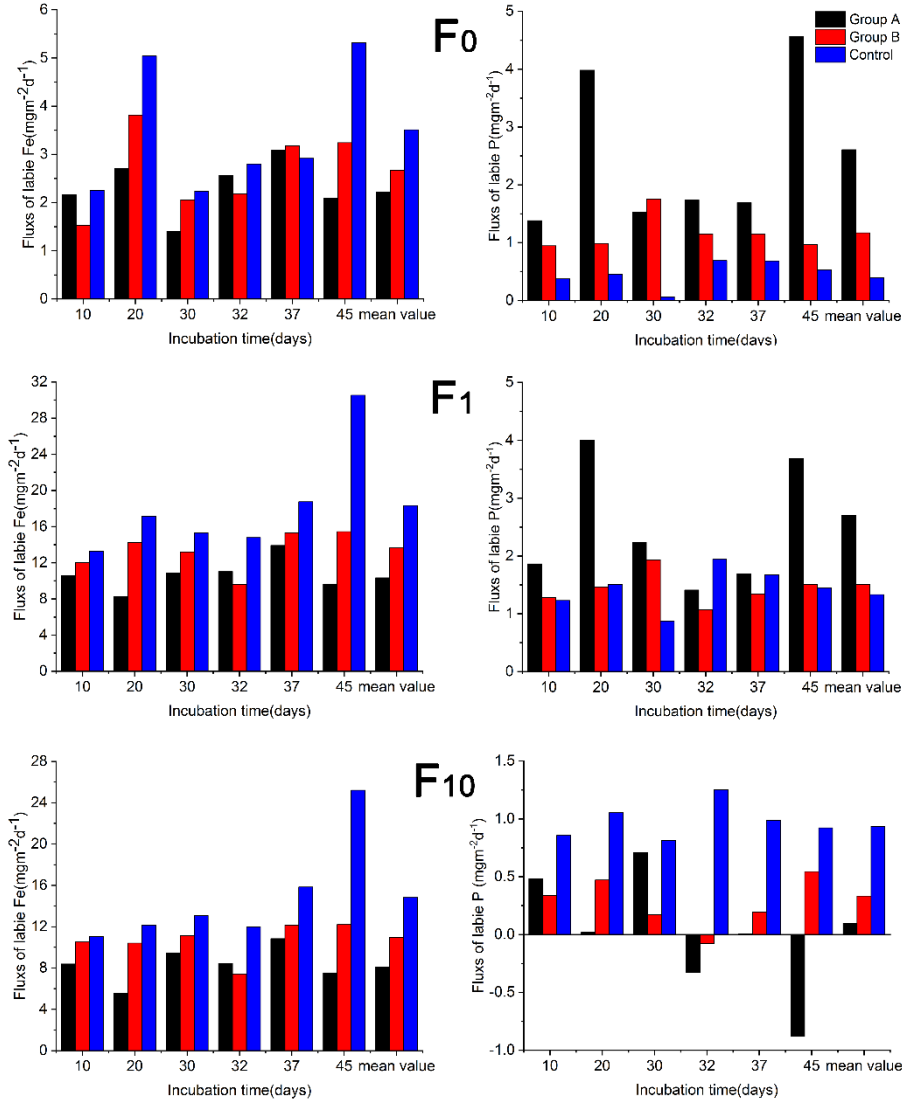


Figure. 6 the apparent diffusive fluxes of  $\text{PO}_4^{3-}$  and  $\text{Fe}^{2+}$  in different treatments. The label  $F_0$  represents the diffusive flux of  $\text{PO}_4^{3-}$  and  $\text{Fe}^{2+}$  from surface sediments to water.  $F_1$  represents the diffusive flux of  $\text{PO}_4^{3-}$  and  $\text{Fe}^{2+}$  from deep to surface sediments.  $F_{10}$  ( $F_{10}=F_1-F_0$ ) is net flux of  $\text{PO}_4^{3-}$  and  $\text{Fe}^{2+}$  in surface sediment. The mean flux of each group represents the average flux during the 45-days incubation period. The mean values of fluxes given here were calculated

according to the following equation: 
$$\bar{F} = \frac{\sum_{i=1}^6 (F_i \times t_i)}{\sum_{i=1}^6 t_i}$$

Where  $\bar{F}$  is the average flux during the 45-days incubation ( $\text{mg m}^{-2} \text{d}^{-1}$ ),  $F_i$  is the flux on the  $i^{\text{th}}$  sampling day ( $\text{mgm}^{-2} \text{d}^{-1}$ ),  $t_i$  is the time interval from the  $(i-1)^{\text{th}}$  sampling day to the  $i^{\text{th}}$  sampling day (day). Control:  $970 \mu\text{M}$ ; group B: low sulfate,  $1,770 \mu\text{M}$ ; group A: high sulfate,  $2,600 \mu\text{M}$ .

### 3.6. Relationship between sulfate concentration and internal P release

Based on the fluxes of labile Fe and P at six sampling times across the SWI ( $F_0$ ) and 1 cm below the SWI ( $F_1$ ), we constructed the diagram for sulfate (Figure. 7). The fluxes of labile P from deep to surface sediments ( $F_1$ ) were all positive. Furthermore, a 100  $\mu\text{M}$  increase of sulfate in overlying water, compared to the concentration of sulfate in the Control group, would induce a  $0.128 \text{ mgm}^{-2}\text{d}^{-1}$  increase of P flux from surface sediment to the overlying water (Figure. S8).

When the concentrations of sulfate were less than 646  $\mu\text{M}$  (Part I in the diagram), the flux of labile P across the SWI was negative. When the concentration increased from 646 to 2,375  $\mu\text{M}$  (Part II), the difference between  $F_1$  and  $F_0$  of labile P gradually reduced to zero. When the concentration of sulfate further increased to more than 2,375  $\mu\text{M}$  (Part III),  $F_0$  of labile P was larger than  $F_1$ . The flux of labile Fe at two depths, over the whole concentration range of sulfate (0 to 3,000  $\mu\text{M}$ ), were all positive and  $F_0$  was always less than  $F_1$ . In addition, the difference between  $F_0$  and  $F_1$  of labile Fe continuously decreased with the increase of sulfate in overlying water.

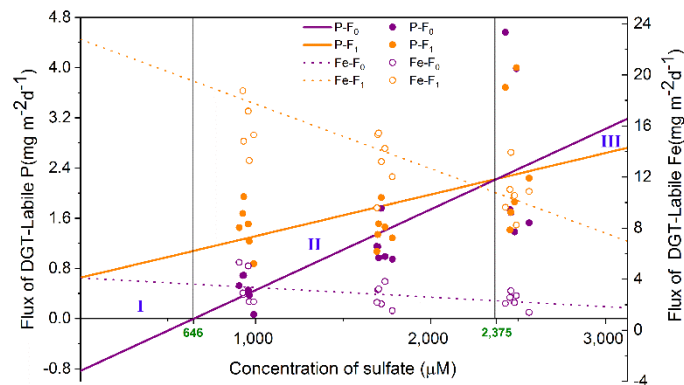


Figure. 7. The functional relation between the apparent diffusive fluxes of  $\text{PO}_4^{3-}(\text{Fe}^{2+})$  and sulfate in overlying water within a concentration range of 0-3,000  $\mu\text{M}$ . The label  $F_0$  represents

the diffusive flux of  $\text{PO}_4^{3-}$  and  $\text{Fe}^{2+}$  from surface sediment to overlying water and  $F_1$  represents the diffusive flux from deep to surface sediments.

## 4. Discussion

### 4.1. Effects of sulfate elevation on the internal P release

It has been reported that elevated sulfate concentrations in freshwaters systems with intermediate concentrations of sulfate ( $>100 \mu\text{M}$ ), greatly promoted the release of internal P under anoxic conditions (Caraco et al. 1989, 1993, Chen et al. 2016a). As for under oxic conditions, Zak et al. (2006) found that increasing sulfate affected the mobilization of P in a lowland freshwater river polluted by mining activities with extremely high concentrations of sulfate (2,600-7,800  $\mu\text{M}$ ). Those concentrations of sulfate are typical of the concentration range ( $\sim 3,000$ -30,000  $\mu\text{M}$ ) of salt waters (Caraco et al. 1989). Here, we additionally found that sulfate with modest concentrations (970-2,600  $\mu\text{M}$ ) promoted release of P under oxic conditions across the SWI.

A higher concentration of SRP in the overlying water was observed with an increase in sulfate (Figure. 4 and Figure. S3). At the end of experiment, the mean concentrations of SRP in sediment pore water from the SWI to -8 cm were 52.3% and 48.6% greater in the group A and group B, respectively, when compared to the Control group (Figure. 4). In addition, P fluxes at the SWI were all positive, which suggested that P was released from surface sediments to the water column (Figure.6). P fluxes from deep to surface sediments (Figure.6) were also positive ( $F_1$  of P  $>0$ ) and larger than the corresponding fluxes from surface sediment to water, indicating that P released from



the oxic surface sediment mainly originated from deeper sediment. Compared with our results under oxic conditions, the maximum concentration of SRP in overlying water under anoxic environments was one order of magnitude higher and the released P was mainly from surface sediments (Chen et al. 2016a, Han et al. 2015). These results demonstrated that redox conditions clearly influenced the mechanisms of sulfate-promoted release of internal P.

#### *4.2. Mechanisms of sulfate-promoted release of internal P*

The process of sulfate-promoted internal P release is closely linked to the reduction of sulfate in sediments (Caraco et al. 1989, Roden and Edmonds 1997, Rozan et al. 2002, Zak et al. 2006). Higher concentrations of labile S below -3cm (Figure. 3b) were observed in group A, which can be mainly attributed to the increase of sulfate in overlying water triggering more sulfate penetration and reduction in the deep sediment. The fluxes of P from deep to surface sediments increased along with the increase of sulfate in water column (Figure. 6). This result agreed well with the previous report that P mobilization is ultimately dependent on the concentration of S(-II) (Zhao et al. 2019). Usually, the source of sulfide is mainly controlled by the reduction of sulfate (Motelica-Heino et al. 2003), which, in freshwater sediments, is regulated by many factors, such as dissolved oxygen, organic matter and concentration of sulfate (Leonov and Chicherina 2008). Here, below the depth of -1 cm, oxygen was exhausted (Figure. 2a) and ORP values decreased to <100 mV (Figure. 2c) in all three groups, which suggested that deep sediment became anoxic and conditions were suitable for sulfate reduction.

The rate of sulfate reduction has been reported as a diffusion-limited, first-order rate process and dependent on initial sulfate concentration (Loh et al. 2013). In our study, increasing concentrations of sulfate in the overlying water led to higher concentrations of sulfate in the pore water (Figure. 3a), which may have accounted for the enhanced activity of sulfate reduction in the deeper, anoxic layers of sediment.

In addition to influencing sulfate reduction in the sediments, higher concentrations of sulfate in the overlying water will also influence the dynamics of Fe(II) in the sediment (Figure. 6). The positive correlations ( $p < 0.001$ ) between labile Fe(II) and labile P (Figure.S7) in each treatment that suggested coincident distributions of labile Fe and labile P existed in the sediment. These coincident distributions with depth should be a result of the reduction of the P-bearing Fe(III)(oxyhydr)oxides (Ding et al. 2012, Xu et al. 2012). The reduction of Fe(III)(oxyhydr)oxides in sediments to Fe(II), is a basic pattern for the P mobilization from sediment to water (Christophoridis and Fytianos 2006). The Fe(II) produced can be maintained in the deep sediment through the formation as iron sulfide coupled with sulfate reduction (Roden and Edmonds 1997). For instance, even under sulfate concentrations limited to 200  $\mu\text{M}$ , sulfide-mediated chemical iron reduction (SCIR) in freshwater systems is a dominate pathway of iron reduction (Hansel et al. 2015). The reduced Fe(II) could precipitate as sulfides via SCIR or directly react with S(-II) in the pore water other than getting back into pore water (Kwon et al. 2014, Lehtoranta et al. 2009). These coincide with our observations that the concentration range of labile Fe (Figure. 5) and fluxes of labile Fe from deep

sediment to surface sediment (Figure. 6) were both decreased in high sulfate system (group A) under a higher concentration of S(-II). Thus, the upward diffusive fluxes of Fe(II) from deep to surface sediments in high sulfate systems were reduced by enhanced sulfate reduction. This resulted in less Fe(II) and sulfide diffusing to the surface oxidized layer as Fe(II) precipitation as sulfides occurred in the deep sediments. Therefore, fewer reducing substances would consume oxygen already present in sediment in High sulfate systems, supporting the observation that a better-oxidized condition existed in surface sediments and that higher DO concentrations across the SWI were found in group A and group B systems compared to the Control (Figure. 2a).

In this study, the oxygen penetration depth (OPD) varied from 0.48 to 0.78 cm (Figure.2b), suggesting that an oxidized layer existed in the surface sediment. Under natural conditions, a thin oxidized layer may exist in surficial sediment in shallow waters, where it can easily be further oxygenated by hydrodynamic disturbance (Chatelain and Guizien 2010). Oxidic conditions are important for iron to maintain its oxidized state, which, in turn, correlates with P retention in sediments (Mortimer 1942). The OPD regulates the thickness of the oxic layer (Wang et al. 2014), a higher thickness decreasing the P release from sediment to overlying water (McManus et al. 1997). However, a higher concentration of SRP released from surface sediment to water was observed in the High sulfate (group A) system (Figure. 4 and Figure. 6). These results suggested that even the deeper OPD of around several millimeters might not be enough to retain the excessive P released from sediment to water induced by elevated sulfate.

Most of the upward diffused Fe(II) in each group (retention efficiencies of Fe(II) varied from 78.5% to 80.8%) was oxidized and retained in surface sediment (Figure. 6) as the oxidation of Fe(II) by oxygen is a rapid process (Chen et al. 2015). Lower fluxes of Fe(II) from deep to surface sediment in the higher sulfate level systems resulted in a lower P-retaining capacity in surface sediments. The decreased ratio of labile Fe to P in sediment associated with higher sulfate also suggested higher sulfate lowered the P retaining capacity (Figure. S7). Therefore, the fluxes of Fe(II), rather than oxygen, were responsible for the larger release of P in more concentrated sulfate systems.

#### *4.3. Concentration effect of sulfate on internal P release*

In this study, we found that increasing sulfate could promote internal P release in eutrophic waters and have the potential to switch sediments between P source and sink, if factors other than sulfate concentration are not considered (Figure.7). **The control of P and sulfate concentration in water were both necessary.** Thus, it is important to quantify the effects of sulfate concentration on internal P release under oxic conditions across the SWI in any given freshwater system.

That the fluxes of P from deep to surface sediments were all positive ( $F_1$  of  $P > 0$ ) suggesting that, in some eutrophic waters, P release from deep sediments might be inevitable. When concentrations of sulfate were lower than 646  $\mu\text{M}$ , well-oxidized conditions across the SWI would be effective for sediment retention of P ( $F_0$  of  $P < 0$ ). However, at sulfate levels  $> 646 \mu\text{M}$ , a 100  $\mu\text{M}$  increase of sulfate in overlying water would result in a  $0.128 \text{ mgm}^{-2}\text{d}^{-1}$  increase in P flux from the sediment to the water

column. In this case, just maintaining a thin oxidized layer (<1 cm) in surface sediment would not be sufficient to control internal P release, as enhanced sulfate reduction limited the Fe(II) release from deep to surface sediments. Once sulfate increased to more than 2,375  $\mu\text{M}$ , the retention capacity for P in the oxidized layer would be exhausted and surface sediment would become another source of P to be released to overlying water. Furthermore, increasing concentrations of sulfate, would gradually reduce the upward diffusion of Fe(II) from the deep sediment, decreasing the production of new adsorption sites for P in surface sediments.

#### *4.4. Environmental implications*

Previous studies reporting that sulfate could induce the release of P from sediment mainly focused on anoxic conditions (Caraco et al. 1993, Chen et al. 2016a, Han et al. 2015, Roden and Edmonds 1997). However, a thin oxidized layer usually exists in surficial sediments in shallow waters and anoxic conditions might not persist during most seasons except over the algal bloom period. In this study, we found that, under oxic conditions across the SWI with modest concentrations of sulfate in eutrophic freshwater, increasing sulfate levels could also promote the release of P from the sediment. The release of internal P induced by sulfate under oxic conditions across the SWI was one magnitude less than in anoxic environments. However, as cyanobacteria have a higher affinity for P, situations with these low concentrations and continuously-released phosphorus from sediment may still contribute to eutrophication and even production of algal blooms (Prentice et al. 2015). **Sediments served as a source for the**

P supply in the water column used by cyanobacteria, and such a process was activated greatly by the higher concentration of sulfate, which pumped up more P from the sediments. More importantly, the intensity of P release was directly influenced by the concentration of sulfate in overlying water and the flux of Fe(II) was the primary factor responsible for P retention. Therefore, as oxygen penetration depth in natural sediments is limited, just improving or maintaining the oxygen level in bottom water may alone be insufficient ~~to control internal P release in a high sulfate ecosystem~~. Technologies aim to increase the depth of oxygen penetration in sediment, suppress the sulfate reduction, or provide new adsorption sites in sediment would be promising for the control internal P release in a high sulfate ecosystem.

## 5. Conclusions

This study investigated the effect of increasing sulfate in shallow waters on internal P release under oxic conditions across the SWI. Higher concentrations of sulfate increased the concentration of SRP in both overlying and pore waters. In addition, higher concentrations of sulfate in overlying water induced a significant increase of labile S(-II) in deep sediment, indicating that enhanced sulfate penetration and reduction occurred in deeper layers of sediment. The fluxes of labile Fe and P from deep to surface sediments were positive and greater than the corresponding fluxes from surface sediment to water column, suggesting that reduction of P-bearing Fe(III)(oxyhydr)oxides in deep sediment acted as a major source for internal P release under oxic conditions across the SWI. Lower fluxes of Fe(II) from deep to surface

566 sediments were found in the High sulfate experimental system, resulting in less re-  
567 oxidized Fe(III) in surface sediments. However, induced by the elevated sulfate, more  
568 P released from deep sediment to surface sediment inevitably resulted in an increase in  
569 the flux of P across the SWI. The results indicated that the influence of sulfate on  
570 internal P released depended largely on the concentrations of sulfate. When the  
571 concentration of sulfate was larger than ca. 646  $\mu\text{M}$ , a 100  $\mu\text{M}$  increase of sulfate  
572 induced a 0.128  $\text{mgm}^{-2}\text{d}^{-1}$  increase of P flux from surface sediment to water column.  
573 Therefore, sulfate concentrations should be considered and controlled for the  
574 management of eutrophic waters.

## 575 **Acknowledgements**

576 The research was supported by the National Key Research and Development Program  
577 of China (2017YFA0207204); the National Natural Science Foundation of China  
578 (41877473, 41401551); and Natural Science Foundation of Beijing (8162040).

## 579 **References**

- 580 Bostrom, B., Andersen, J.M., Fleischer, S. and Jansson, M. (1988) Exchange of Phosphorus  
581 across the Sediment - Water Interface. *Hydrobiologia* 170, 229-244.
- 582 Caraco, N.F., Cole, J.J. and Likens, G.E. (1989) Evidence for Sulfate-Controlled Phosphorus  
583 Release from Sediments of Aquatic Systems. *Nature* 341(6240), 316-318.
- 584 Caraco, N.F., Cole, J.J. and Likens, G.E. (1993) Sulfate Control of Phosphorus Availability in  
585 Lakes - a Test and Reevaluation of Hasler and Einsele Model. *Hydrobiologia* 253(1-3), 275-

586        280.

587     Carpenter, S.R. (2008) Phosphorus control is critical to mitigating eutrophication. Proceedings  
588        of the National Academy of Sciences of the United States of America 105(32), 11039-11040.

589     Chatelain, M. and Guizien, K. (2010) Modelling coupled turbulence - Dissolved oxygen  
590        dynamics near the sediment-water interface under wind waves and sea swell. Water  
591        Research 44(5), 1361-1372.

592     Chen, M., Ding, S., Liu, L., Xu, D., Han, C. and Zhang, C. (2015) Iron-coupled inactivation of  
593        phosphorus in sediments by macrozoobenthos (chironomid larvae) bioturbation: Evidences  
594        from high-resolution dynamic measurements. Environmental Pollution 204, 241-247.

595     Chen, M., Li, X.H., He, Y.H., Song, N., Cai, H.Y., Wang, C.H., Li, Y.T., Chu, H.Y., Krumholz,  
596        L.R. and Jiang, H.L. (2016a) Increasing sulfate concentrations result in higher sulfide  
597        production and phosphorous mobilization in a shallow eutrophic freshwater lake. Water  
598        Research 96, 94-104.

599     Chen, M.S., Ding, S.M., Liu, L., Xu, D., Gong, M.D., Tang, H. and Zhang, C.S. (2016b)  
600        Kinetics of phosphorus release from sediments and its relationship with iron speciation  
601        influenced by the mussel (*Corbicula fluminea*) bioturbation. Science of the Total  
602        Environment 542, 833-840.

603     Christophoridis, C. and Fytianos, K. (2006) Conditions affecting the release of phosphorus from  
604        surface lake sediments. Journal of Environmental Quality 35(4), 1181-1192.

605     Conley, D.J., Paerl, H.W., Howarth, R.W., Boesch, D.F., Seitzinger, S.P., Havens, K.E.,  
606        Lancelot, C. and Likens, G.E. (2009) ECOLOGY Controlling Eutrophication: Nitrogen and



607 Phosphorus. *Science* 323(5917), 1014-1015.

608 Coveney, M.F., Lowe, E.F., Battoe, L.E., Marzolf, E.R. and Conrow, R. (2005) Response of a  
609 eutrophic, shallow subtropical lake to reduced nutrient loading. *Freshwater Biology* 50(10),  
610 1718-1730.

611 Ding, S., Han, C., Wang, Y., Yao, L., Wang, Y., Xu, D., Sun, Q., Williams, P.N. and Zhang, C.  
612 (2015) In situ, high-resolution imaging of labile phosphorus in sediments of a large  
613 eutrophic lake. *Water Research* 74, 100-109.

614 Ding, S.M., Sun, Q., Xu, D., Jia, F., He, X. and Zhang, C.S. (2012) High-Resolution  
615 Simultaneous Measurements of Dissolved Reactive Phosphorus and Dissolved Sulfide: The  
616 First Observation of Their Simultaneous Release in Sediments. *Environmental Science &*  
617 *Technology* 46(15), 8297-8304.

618 Gächter, R. and Müller, B. (2003) Why the Phosphorus Retention of Lakes Does Not  
619 Necessarily Depend on the Oxygen Supply to Their Sediment Surface. *Limnology &*  
620 *Oceanography* 48(2), 929-933.

621 Gao, Y., Liang, T., Tian, S., Wang, L., Holm, P.E. and Hansen, H.C.B. (2016) High-resolution  
622 imaging of labile phosphorus and its relationship with iron redox state in lake sediments.  
623 *Environmental Pollution* 219, 466-474.

624 Han, C., Ding, S.M., Yao, L., Shen, Q.S., Zhu, C.G., Wang, Y. and Xu, D. (2015) Dynamics of  
625 phosphorus-iron-sulfur at the sediment-water interface influenced by algae blooms  
626 decomposition. *Journal of Hazardous materials* 300, 329-337.

627 Hansel, C.M., Lentini, C.J., Tang, Y.Z., Johnston, D.T., Wankel, S.D. and Jardine, P.M. (2015)

628 Dominance of sulfur-fueled iron oxide reduction in low-sulfate freshwater sediments. *Isme*  
629 *Journal* 9(11), 2400-2412.

630 Higashino, M. (2011) Oxygen consumption by a sediment bed for stagnant water: Comparison  
631 to SOD with fluid flow. *Water Research* 45(15), 4381-4389.

632 Huser, B.J., Futter, M.N., Wang, R. and Fölster, J. (2018) Persistent and widespread long-term  
633 phosphorus declines in Boreal lakes in Sweden. *Science of the Total Environment* 613-614,  
634 240-249.

635 Jilbert, T., Slomp, C.P., Gustafsson, B.G. and Boer, W. (2011) Beyond the Fe-P-redox  
636 connection: preferential regeneration of phosphorus from organic matter as a key control  
637 on Baltic Sea nutrient cycles. *Biogeosciences* 8(6), 1699-1720.

638 Kraal, P., Burton, E.D., Rose, A.L., Cheetham, M.D., Bush, R.T. and Sullivan, L.A. (2013)  
639 Decoupling between Water Column Oxygenation and Benthic Phosphate Dynamics in a  
640 Shallow Eutrophic Estuary. *Environmental Science & Technology* 47(7), 3114-3121.

641 Kwon, M.J., Boyanov, M.I., Antonopoulos, D.A., Brulc, J.M., Johnston, E.R., Skinner, K.A.,  
642 Kemner, K.M. and O'Loughlin, E.J. (2014) Effects of dissimilatory sulfate reduction on  
643 FeIII (hydr)oxide reduction and microbial community development. *Geochimica et*  
644 *Cosmochimica Acta* 129, 177-190.

645 Lehtoranta, J., Ekholm, P. and Pitkanen, H. (2009) Coastal Eutrophication Thresholds: A Matter  
646 of Sediment Microbial Processes. *Ambio* 38(6), 303-308.

647 Leonov, A.V. and Chicherina, O.V. (2008) Sulfate reduction in natural water bodies. 1. The  
648 effect of environmental factors and the measured rates of the process. *Water Resources*

649 35(4), 417-434.

650 Li, Y.H. and Gregory, S. (1974) DIFFUSION OF IONS IN SEA-WATER AND IN DEEP-SEA  
651 SEDIMENTS. *Geochimica et Cosmochimica Acta* 38(5), 703-714.

652 Loh, P.S., Molot, L.A., Nuernberg, G.K., Watson, S.B. and Ginn, B. (2013) Evaluating  
653 relationships between sediment chemistry and anoxic phosphorus and iron release across  
654 three different water bodies. *Inland Waters* 3(1), 105-118.

655 McManus, J., Berelson, W.M., Coale, K.H., Johnson, K.S. and Kilgore, T.E. (1997) Phosphorus  
656 regeneration in continental margin sediments. *Geochimica et Cosmochimica Acta* 61(14),  
657 2891-2907.

658 Mortimer, C.H. (1942) The exchange of dissolved substances between mud and water in lakes.  
659 *Journal of Ecology* 30, 147-201.

660 Motelica-Heino, M., Naylor, C., Zhang, H. and Davison, W. (2003) Simultaneous release of  
661 metals and sulfide in lacustrine sediment. *Environmental Science & Technology* 37(19),  
662 4374-4381.

663 Murphy, J. and Riley, J.P. (1962) A modified single solution method for the determination of  
664 phosphate in natural waters. *Analytica Chimica Acta* 27, 31-36.

665 Paerl, H.W., Hall, N.S. and Calandrino, E.S. (2011) Controlling harmful cyanobacterial blooms  
666 in a world experiencing anthropogenic and climatic-induced change. *Science of the Total*  
667 *Environment* 409(10), 1739-1745.

668 Paytan, A., Roberts, K., Watson, S., Peek, S., Chuang, P.C., Defforey, D. and Kendall, C. (2017)  
669 Internal loading of phosphate in Lake Erie Central Basin. *Science of the Total Environment*

670 579, 1356-1365.

671 Prentice, M.J., OBrien, K.R., Hamilton, D.P. and Burford, M.A. (2015) High- and low-affinity  
672 phosphate uptake and its effect on phytoplankton dominance in a phosphate-depauperate  
673 lake. *Aquatic Microbial Ecology* 75(2), 139-153.

674 Qin, B.Q., Xu, P.Z., Wu, Q.L., Luo, L.C. and Zhang, Y.L. (2007) Environmental issues of Lake  
675 Taihu, China. *Hydrobiologia* 581, 3-14.

676 Roden, E.E. and Edmonds, J.W. (1997) Phosphate mobilization in iron-rich anaerobic  
677 sediments: Microbial Fe(III) oxide reduction versus iron-sulfide formation. *Archiv Fur*  
678 *Hydrobiologie* 139(3), 347-378.

679 Rozan, T.F., Taillefert, M., Trouwborst, R.E., Glazer, B.T., Ma, S.F., Herszage, J., Valdes, L.M.,  
680 Price, K.S. and Luther, G.W. (2002) Iron-sulfur-phosphorus cycling in the sediments of a  
681 shallow coastal bay: Implications for sediment nutrient release and benthic macroalgal  
682 blooms. *Limnology and Oceanography* 47(5), 1346-1354.

683 Rydin, E. (2000) Potentially mobile phosphorus in Lake Erken sediment. *Water Research* 34(7),  
684 2037-2042.

685 Schindler, D.W., Hecky, R.E., Findlay, D.L., Stainton, M.P., Parker, B.R., Paterson, M.J., Beaty,  
686 K.G., Lyng, M. and Kasian, S.E.M. (2008) Eutrophication of lakes cannot be controlled by  
687 reducing nitrogen input: Results of a 37-year whole-ecosystem experiment. *Proceedings of*  
688 *the National Academy of Sciences of the United States of America* 105(32), 11254-11258.

689 Smith, V.H. (2003) Eutrophication of freshwater and coastal marine ecosystems - A global  
690 problem. *Environmental Science and Pollution Research* 10(2), 126-139.

691 Sun, Q., Ding, S.M., Zhang, L.P., Chen, M.S. and Zhang, C.S. (2017) A millimeter-scale  
 692 observation of the competitive effect of phosphate on promotion of arsenic mobilization in  
 693 sediments. *Chemosphere* 180, 285-294.

694 Tabatabai, M.A. (1974) A Rapid Method for Determination of Sulfate in Water Samples.  
 695 *Environmental Letters* 7(3), 237-243.

696 Tong, Y., Zhang, W., Wang, X., Couture, R.M., Larssen, T., Zhao, Y., Li, J., Liang, H., Liu, X.  
 697 and Bu, X. (2017) Decline in Chinese lake phosphorus concentration accompanied by shift  
 698 in sources since 2006. *Nature Geoscience* 10(7), 12-2017.

699 Ullman, W.J. and Aller, R.C. (1982) Diffusion-Coefficients in Nearshore Marine-Sediments.  
 700 *Limnology and Oceanography* 27(3), 552-556.

701 Wang, C., Shan, B., Zhang, H. and Rong, N. (2014) Analyzing sediment dissolved oxygen  
 702 based on microprofile modeling. *Environmental Science and Pollution Research* 21(17),  
 703 10320-10328.

704 Wang, Y., Ding, S.M., Wang, D., Sun, Q., Lin, J., Shi, L., Chen, M.S. and Zhang, C.S. (2017)  
 705 Static layer: A key to immobilization of phosphorus in sediments amended with lanthanum  
 706 modified bentonite (Phoslock (R)). *Chemical Engineering Journal* 325, 49-58.

707 Xu, D., Chen, Y.F., Ding, S.M., Sun, Q., Wang, Y. and Zhang, C.S. (2013) Diffusive Gradients  
 708 in Thin Films Technique Equipped with a Mixed Binding Gel for Simultaneous  
 709 Measurements of Dissolved Reactive Phosphorus and Dissolved Iron. *Environmental*  
 710 *Science & Technology* 47(18), 10477-10484.

711 Xu, D., Wu, W., Ding, S.M., Sun, Q. and Zhang, C.S. (2012) A high-resolution dialysis

712 technique for rapid determination of dissolved reactive phosphate and ferrous iron in pore  
 713 water of sediments. *Science of the Total Environment* 421, 245-252.

714 Yu, T., Zhang, Y., Wu, F.C. and Meng, W. (2013) Six-Decade Change in Water Chemistry of  
 715 Large Freshwater Lake Taihu, China. *Environmental Science & Technology* 47(16), 9093-  
 716 9101.

717 Zak, D., Kleeberg, A. and Hupfer, M. (2006) Sulphate-mediated phosphorus mobilization in  
 718 riverine sediments at increasing sulphate concentration, River Spree, NE Germany.  
 719 *Biogeochemistry* 80(2), 109-119.

720 Zhao, Y.P., Zhang, Z.Q., Wang, G.X., Li, X.J., Ma, J., Chen, S., Deng, H. and Annalisa, O.H.  
 721 (2019) High sulfide production induced by algae decomposition and its potential  
 722 stimulation to phosphorus mobility in sediment. *Science of the Total Environment* 650, 163-  
 723 172.

724 Zilius, M., De Wit, R. and Bartoli, M. (2016) Response of sedimentary processes to  
 725 cyanobacteria loading. *Journal of limnology* 75(2), 236-247.

726

727